A Comparison of Aerosol and Momentum Mixing in Dust Storms Using Fast-Response Instruments

WILLIAM M. PORCH

Lawrence Livermore Laboratory, University of California,[1] Livermore, Calif. 94550

DALE A. GILLETTE

National Center for Atmospheric Research,[2] Boulder, Colo. 80307

(Manuscript received 2 May 1977, in revised form 2 September 1977)

ABSTRACT

Fast-response light scattering measurements at two heights during a Texas dust storm are combined with horizontal and vertical wind data to derive and compare aerosol flux estimates using three techniques. The major result of this study is that a relative equivalence exists between the fine-particle (0.1 μm < radius < 1 μm) exchange coefficient and the eddy viscosity of the wind. The data also shed some light on the complex dependence of wind speed threshold for suspension and aerosol flux in high winds for different surface conditions and soil types. These results show the value of the experimental technique to studies of toxic particulate suspension and deposition by wind.

1. Introduction

Studies of windblown particles have a rich history with a wide variety of motivations. These studies include agricultural and geological investigations of erosion and sand and mixed soils (Bagnold, 1941; Chepil, 1957; Skidmore, 1974), nuclear hazards investigations of resuspension of radioactive particles (Anspaugh *et al.*, 1973; Sehmel and Lloyd, 1976), windblown snow (Businger, 1965; Mellor, 1965), dispersion of biological material (Raynor, 1976; Aylor, 1976), ocean spray (Bortkovskij, 1972; Heathershaw, 1974), and even refloatation of urban pollution particulates (Newman *et al.*, 1974; Harrison *et al.*, 1976). Investigations have been made in wind tunnels (Punjrath and Heldman, 1972) and in the open environment (Carlson *et al.*, 1973; Patterson *et al.*, 1976; Hagen and Woodruff, 1973). Despite these efforts the fine-particulate fluxes from soil surfaces remains a difficult parameter to measure and relate to wind speed, soil type and condition, and the turbulence parameters of the wind.

Our approach to this problem was to combine fast-response aerosol light scattering instrumentation and anemometers with filter samples to resolve the turbulent fluxes of aerosol and wind momentum. The basic experimental design consisted of a vertically displaced pair of integrating nephelometers (Ahlquist and Charlson, 1967) along with several anemometers and at least one measure of the vertical velocity at the height of the nephelometer. Filter samples were also taken at several heights. The principal experiment was conducted in a farm field with loamy soil near Abernathy, Tex., during April 1975. Some measurements were also taken the previous year in a sandy soil field near Plains, Tex. (Porch and Shinn, 1976; Shinn *et al.*, 1976; Gillette, 1976). From the information derived from the above-mentioned instruments we were able to determine the following:

1) A comparison of the aerosol exchange coefficient (K_A) and the eddy viscosity (K_M) for the deposition period.

2) Aerosol deposition velocity and flux, during a dust storm prior to a frontal passage.

3) Spectral analysis of the auto- and cross-spectral densities of the vertical and horizontal wind and the light scattering measurements of dust.

These data can be compared to previous measurements made under different sampling, soil and meteorological conditions.

2. Theory

a. Eddy correlation

The eddy-correlation technique is the most direct technique of turbulent flux determination and involves

[1] Work performed under the auspices of the U. S. Energy Research and Development Administration under Contract W-7405-Eng-48.

[2] The National Center for Atmospheric Research is sponsored by the National Science Foundation.

following the variations of wind speed and light scattering to determine

$$F_A = \overline{b'_{\text{scat}} w'} = -K_A \frac{db_{\text{scat}}}{dz}$$

and

$$\tau = \rho \overline{u'w'} = -\rho K_M \frac{du}{dz}, \quad (1)$$

where u', w', b'_{scat} represent the instantaneous deviation from the mean of horizontal and vertical wind speed and aerosol light scatter, respectively, τ is the shearing stress and ρ the air density. In order to determine fluxes with this technique care must be taken to insure that all frequencies important to turbulent transport are detected by the sensor. If a nondimensional frequency is defined as

$$f = nz/\bar{u} \quad (\text{for ideal } f_{\max} \gtrsim 1.5 \text{ and } f_{\min} \gtrsim 0.001), \quad (2)$$

where n, z and $\bar{u}$ are the sampling frequency, the sensor height and the mean wind, respectively, then the range of values of f should be higher than 1.5 and lower than 0.001 for stress and fluxes with the same spectral density as stress (Kaimal, 1975). We will see subsequently from spectral analysis of the data that these criteria were met. When the profile and eddy correlation techniques are combined, Eq. (2) implies that the ratio of K_A to K_M can be determined.

b. *Profile method*

The second and perhaps simplest technique for flux determination is to use the vertical pair of nephelometers and anemometers to define the profile to derive the light scattering aerosol flux as

$$F_A = K_A \frac{\Delta b_{\text{scat}}}{\Delta z}, \quad (3)$$

where b_{scat} is the integrated light scattering coefficient and z the instrument height. F_A can be related to the total (number) flux of particles by the measured size distribution on the filter samples. By assuming equivalence between K_A and K_M, F_A can be determined through the drag coefficient C_d (Gillette *et al.*, 1972). This technique no longer requires the assumption of steady state, but does require the speed of response necessary for the application of the eddy-correlation technique.

c. *Calculation of deposition velocity*

A third method of determining the vertical flux of aerosols is to use the deposition velocity concept in which the vertical flux of an air additive is equal to the average concentration at a given height multiplied by a deposition velocity. The deposition velocity is computed from

$$F_A = \bar{C}\sigma_w \int_{-\infty}^{\infty} xF(x)P(x)dx, \quad (4)$$

where $\bar{C}$ is the mean concentration at the sampling height z; σ_w is the standard deviation of the vertical velocity fluctuations,

$$x = \frac{w - \bar{w}}{\sigma_w},$$

where w is the instantaneous value of the vertical wind; and

$$F(x) = \frac{C(x)}{\bar{C}},$$

where $C(x)$ is the mean value of a concentration for a given value of the vertical wind expressed in terms of x, and $P(x)$ is the probability distribution of x.

In the present treatment the assumption used was that $\sigma_w = Au_*$, where u_* is the friction velocity and A a constant (Lumley and Panofsky, 1964; Wyngaard *et al.*, 1971). The time series of vertical wind $w(+)$ and $b_{\text{scat}}(+)$ were used to construct the functions $F(x)$ and $P(x)$. The approximation was used that

$$F(x) = \frac{b_{\text{scat}}(x)}{\overline{b_{\text{scat}}}}. \quad (5)$$

That is, b_{scat} was assumed proportional to mass loading of aerosol. The probability distribution for w was nearly Gaussian, and the value of the integral

$$C_A = \int_{-\infty}^{\infty} xF(x)P(x)dx \quad (6)$$

was determined numerically. The vertical light scattering aerosol flux can then be determined as

$$F_A = \bar{C}u_* A C_A, \quad (7)$$

where A is usually close to unity. That is, the light scattering particle flux is a product of mean concentration multiplied by a deposition velocity that is equal to a friction velocity times a constant C_A. The results of this and the previous two techniques will be developed after a description of the experimental conditions.

3. Experimental conditions

The primary experiment was located on erodible soil in a farm field near Abernathy, Tex. The land was denuded of vegetation with vegetative residue in the amount 144 g m^{-2}. The soil was dry with 1.9% soil

moisture by weight and was relatively loose with 51% of the mass in aggregates smaller than 0.84 mm. The soil was a flat exposure of Estacado loam with a surface texture sandy clay loam determined by the Buoycous method (Buoycous, 1951). A slightly furrowed structure of the soil remained with furrow-to-ridge-height differences averaging about 3 cm. The instrumentation was located on a 5 m tower west of a north-south dirt road on the same Estacado soil having a smoother surface and less coherent aggregates structure. Filter samples were collected about 40 m south of the tower. The fetch-to-height sampling ratio was greater than 10 for the conditions of this experiment.

The instrumentation on the tower consisted of two integrating nephelometers (Ahlquist and Charlson, 1967) with cup (Teledyne Geotech model 51.B) and vectorvane anemometers (Meteorological Research Inc. Model 1053) at heights shown in Table 1. Most of the results presented will be from the 5 m nephelometer and vectorvane, yielding the lowest maximum sampling frequency of ~5.25 Hz with an average wind of 19 m s^{-1} from Eq. (3). The nephelometer air flow system was modified to give a flow rate of 472 cm^3 s^{-1} in order to circulate aerosol through the light scattering chamber in less than 0.1 s. The system was run on test mode with aerosol scattering sampled over eight times per second. The subsequent spectral analysis of the nephelometer data shows that the high-frequency response is close to the ideal high-frequency response of 5.25 Hz. A vectorvane provided the wind data. With the distance constant of ~1 m the vectorvane, in 19 m s^{-1} winds, also proved to have a maximum frequency response close to ideal. The data were collected on analog tapes, which were subsequently digitized at 1/20th of a second.

The experiment took place on 7 April 1975. After several days of waiting, wind speeds were sufficient to erode the soil of the road which was more erodible than the field soil. Since winds were southeasterly along a flat area, we were able to sample dust which had blown from the road and which was settling by turbulent diffusion. The high winds averaging about 19 m s^{-1}

TABLE 1. Mean values for light scattering coefficients (b_{scat}), horizontal wind velocity (u), vertical wind velocity (w), azimuth (ϕ) and temperature (T).

Instrument	Parameter	Height (m)	Mean value for period representing Deposition (320 s)	Suspension (100 s)
Nephelometer	b_{scat}	1.4	1.15×10^{-4} m^{-1}	4.48×10^{-4} m^{-1}
		5.1	2.08×10^{-4} m^{-1}	3.60×10^{-4} m^{-1}
Vectorvane anemometer	u	5.4	18.9 m s^{-1}	16.8 m s^{-1}
Cup anemometer	u	1.0	14.23 m s^{-1}	13.0 m s^{-1}
Thermistor	T	5.3	20.3°C	15.7°C
Vectorvane anemometer	w	5.4	~0 m s^{-1}	~0 m s^{-1}
Direction	ϕ		45°	105°

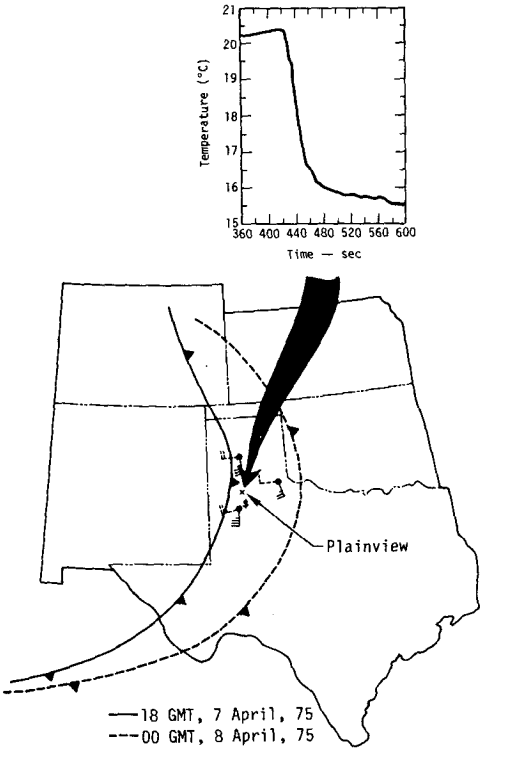

FIG. 1. Movement of a cold front concurrent with the period of measurement near Abernathy, Tex., on 7 April 1976, during a dust storm. The graph in the upper right hand corner shows the rapid drop in temperature associated with the front.

were accompanied by a thick cloud cover and we inferred a nearly neutral atmosphere for the time of the experiment. A wind shift and temperature drop occurred after about 6 min of measurements of dust deposition of previously suspended particles from local and distant roads and fields (our field was not emitting particles). After the wind shift caused by the frontal passage, aerosol began to be raised from our field (see Fig. 1). This reverse in the direction of aerosol flux is evident from the sign of the difference between the light scattering values from the nephelometers at the two heights shown in Fig. 2. Fig. 2 shows the pulse of aerosol from the surface after the wind changed direction (Fig. 2a) along with the wind speed at 1 m (Fig. 2b) and the difference between the upper and lower nephelometers (Fig. 2c). After about 1.5 min a torrential rain and hail storm halted all wind erosion and our experiment. The criterion expressed in Eq. (3) shows that although the sampling period for the eddy-correlation technique was long enough (6 min) for the deposition period, the suspension period was too short for proper application of this technique.

Two factors combine to complicate the relationship between the light scattering coefficient b_{scat} measured at the nephelometer and the aerosol mass concentration and visual range outside the nephelometer. These

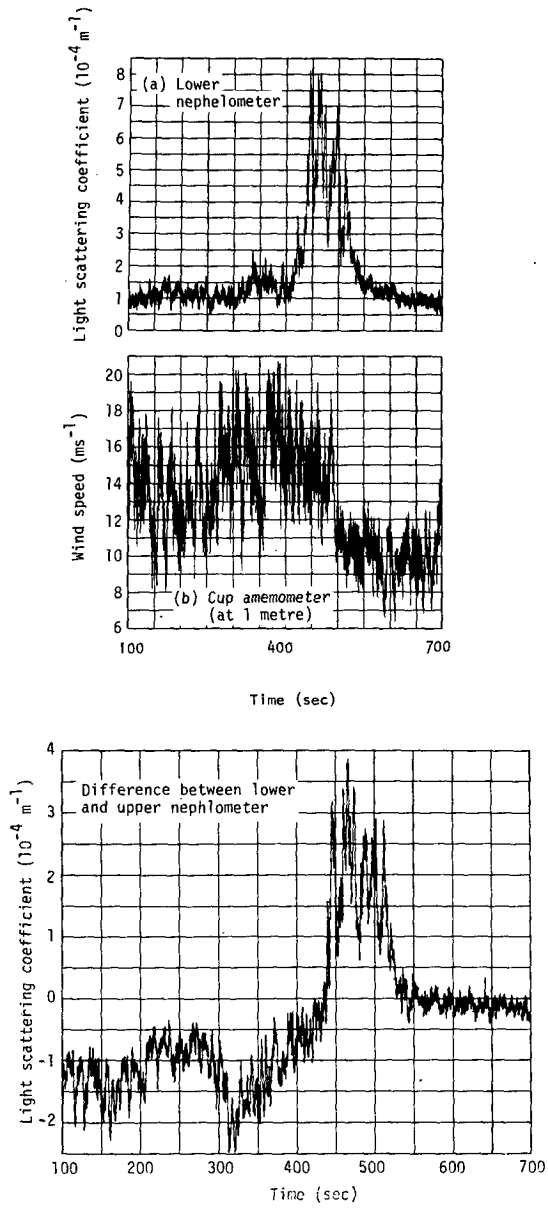

FIG. 2. Comparison of the data taken during the period illustrated in Fig. 1: (a) nephelometer data in light scattering units at 1.4 m; (b) cup anemometer data in meters per second at 1 m; (c) difference between nephelometer at 5.1 m and nephelometer at 1.4 m. The negative values are associated with aerosol deposition and positive values with aerosol suspension.

factors are as follows:

1) The effective loss of large particles, which pass over the vertically oriented sampling tube, because of their inertia. The aspiration ratio, defined as the ratio of aerosol measured through the vertically oriented tube to the ambient concentration, is less than 1 for larger particles and low sample flow rates.

2) The truncation angle effect in the integrating nephelometer, due to the finite size of the instrument and the attendent inability to integrate the light scatter completely to 180° from an angle of exactly 0°. The forward angle truncation reduces the sensitivity to large particle light scatter (to 50% in the limit of very large particles) (Ensor and Waggoner, 1970).

Laktionov (1967) has derived and tested a formula for the aspiration ratio for perpendicular sampling:

$$A_d = 1 - 3K_d^{(V_k/V_b)^{1/2}}, \tag{8}$$

where K_d is the Stokes number for the nephelometer sampling tube as a function of particle diameter d, V_k is the sampling flow velocity and V_b is the horizontal wind flow velocity. Care should be taken not to apply Eq. (8) to Stokes numbers greater than the tested range of between 0.003 and 0.2. (Lundgren). With a 4.6 cm diameter tube and sample flow rate of 472 cm s^{-1} in high winds, the over Stokes number range allows us to apply Eq. (8) to particles with radii between 0.5 and 5 μm. Because the sampling efficiency varies as a function of horizontal wind speed, a correction had to be made to the light scattering values associated with winds less than or greater than average.

The net effect on the sampled aerosol distribution of the factors mentioned in the previous paragraph is shown in Fig. 3. Curve (a) shows a lognormal approximation to the particle size distribution measured with filter samples. This distribution has a geometric mean and standard deviation of 2.5 and 0.6 μm, respectively. Curves (b) and (d) illustrate the effects of the aspiration and truncation angle, respectively. Curve (c) illustrates the combined aspiration and truncation angle effects. These effects were tested directly by alterately sampling straight into the wind and perpendicular to it. Increased scattering was found for horizontal sampling due to the larger particles, which ranged from 30% to 60% depending on the wind speed.

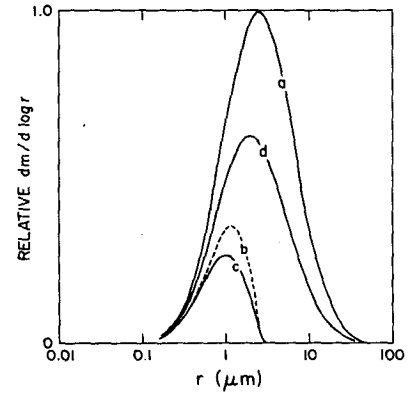

FIG. 3. Effect of anisotropic vertical sampling and angular truncation in the aerosol size distribution sensed by the nephelometer: (a) the "ambient" size distribution; (b) the size distribution "seen" by vertical-pointing nephelometer for the mean wind speed; (c) the size distribution "seen" by the nephelometer for the mean wind speed, corrected for particle size sensitivity of the integrating nephelometer due to the truncation angle effect; (d) the equivalent size distribution due to truncation error reduction of the ambient size distribution.

The time lag for maximum covariance, associated with the amount of time the aerosol takes to flow through the sampling tube and enter the scattering chamber, was about 3 for the deposition period and 5.4 s for the suspension period, which may be caused by the upward aerosol flow opposing the sampling flow of the nephelometer. Also, a slight complication arose when the horizontal wind sensor broke electrical contact at times during this period. These breaks were easily identified by sudden drops to zero. The data were replaced by data from the lower anemometer scaled up to the height of the vectorvane. These breaks occurred in fewer than 10% of the record and lower anemometer and upper anemometer variations correlated by 0.7.

Figs. 2a–2c show data taken before and after the front shown in Fig. 1 passed the observation site. The front arrived at about 420 s into this record at 1358 local time. As previously mentioned, local suspension did not take place until the front passed and the wind changed from south to west-southwest (Fig. 2c). However, Fig. 2b shows that the total wind speed did not increase and in fact decreased slightly during this period. This is the result of increased shearing stress due to the change of wind direction from perpendicular to almost parallel to the field furrows and possibly the increased turbulent energy associated with the front. The increase in shearing stress implies an increase in the friction velocity u_* and turbulent energy has been shown to be important in the suspension process by Punjrath and Heldman (1972).

4. Results

a. K_M vs K_A

The covariances of the wind and dust can be used as independent measure of many of the parameters described in Eq. (2), using the eddy-correlation technique. The length of record of the deposition period is just sufficiently long to use the covariances to determine τ and F_A. Table 1 summarizes the mean value of the parameters measured as a function of height during the deposition and suspension periods before and after the frontal passage. It is possible to obtain a measure of K_M and K_A independently by combining these values for τ and F_A with the differences shown in Table 1 and the equation

$$\frac{K_A}{K_M}=\frac{\overline{b'_{\text{scat}}w'}}{\overline{u'w'}}\frac{\Delta u}{\Delta b_{\text{scat}}}. \tag{9}$$

For the deposition case $\overline{u'w'}$ and $\overline{b'_{\text{scat}}w'}$ were determined to be 0.15 m^2 s^{-2} and 0.03 ($\times 10^{-4}$ s^{-1}), respectively, which results in a ratio of K_M/K_A equal to $\sim$1.0 (a value of 1.0 is usually assumed without measurement) (Gillette *et al.*, 1972).

The time period was too short for comparable analysis to be meaningful during the suspension period. During the suspension period both $\overline{u'w'}$ and $\overline{b'_{\text{scat}}w'}$ increased in magnitude to 0.23 m^2 s^{-2} and -0.08 s^{-1}, respectively. This implied an increase in surface shearing stress and an upward flux of aerosol associated with the frontal passage.

b. *Mean profile data*

Fig. 4 shows scatter plots of the difference between upper and lower nephelometer b_{scat} versus wind speed at 1 m. Figs. 4a and 4b are for the deposition and suspension part of the record, respectively. Fig. 4a shows only a general bunching of values for deposition with wind speeds as high as 20 m s^{-1}. The logarithmic scale plot in Fig. 4b for suspension shows a very noisy relation between wind speed and differences above 0.1×10^{-4}. Fig. 4c shows an analogous record recorded the previous year with sandy soil conditions rather than loam. The two nephelometers that year were closer to the ground at 35.5 and 166 cm (Porch and Shinn, 1976). This scatter plot represents an hour's worth of data with a 30 s filter. The data are much more closely clumped and have an exponential relationship to wind speed for values between 4 and 7 m s^{-1}. These differences are related to the aerosol flux as a function of wind speed through Eq. (1). This high exponential relationship between wind and dust flux has been observed by Gillette (1974) and Sehmel and Lloyd (1976) from filter samples where much longer averaging times are involved. The data in Figs. 4a and 4b would imply a threshold wind velocity for suspension of over 20 m s^{-1} for wind perpendicular to the field furrows and between 10 and 15 m s^{-1} for the more turbulent winds almost parallel to the furrows. These values for loamy soil compare to a value of about 8 m s^{-1} for the previous year in a highly erodible sandy soil field.

c. *Computation of deposition velocities*

The probability distribution of the vertical velocity was then determined for inclusion in Eq. (6) by using the deposition velocity technique. The one-dimensional probability densities for horizontal b_{scat} and vertical wind, using the wind at 5 m during the deposition period, are shown in Fig. 5. The form of $F(x)$ is shown in Fig. 6. C_A was found to be

$$C_A\approx 0.01. \tag{10}$$

With A determined equal to 3.5, Eq. (7) takes the form

$$F_A\approx 0.04u_*\bar{C}. \tag{11}$$

The above expression can be compared to the work of Hicks (1976) and of Sehmel and Hodgson (1976). Hicks approached the calculation of deposition velocities by considering the vertical flux to be a product of a deposition velocity times the difference of concentrations at two heights. An expression given by Hicks

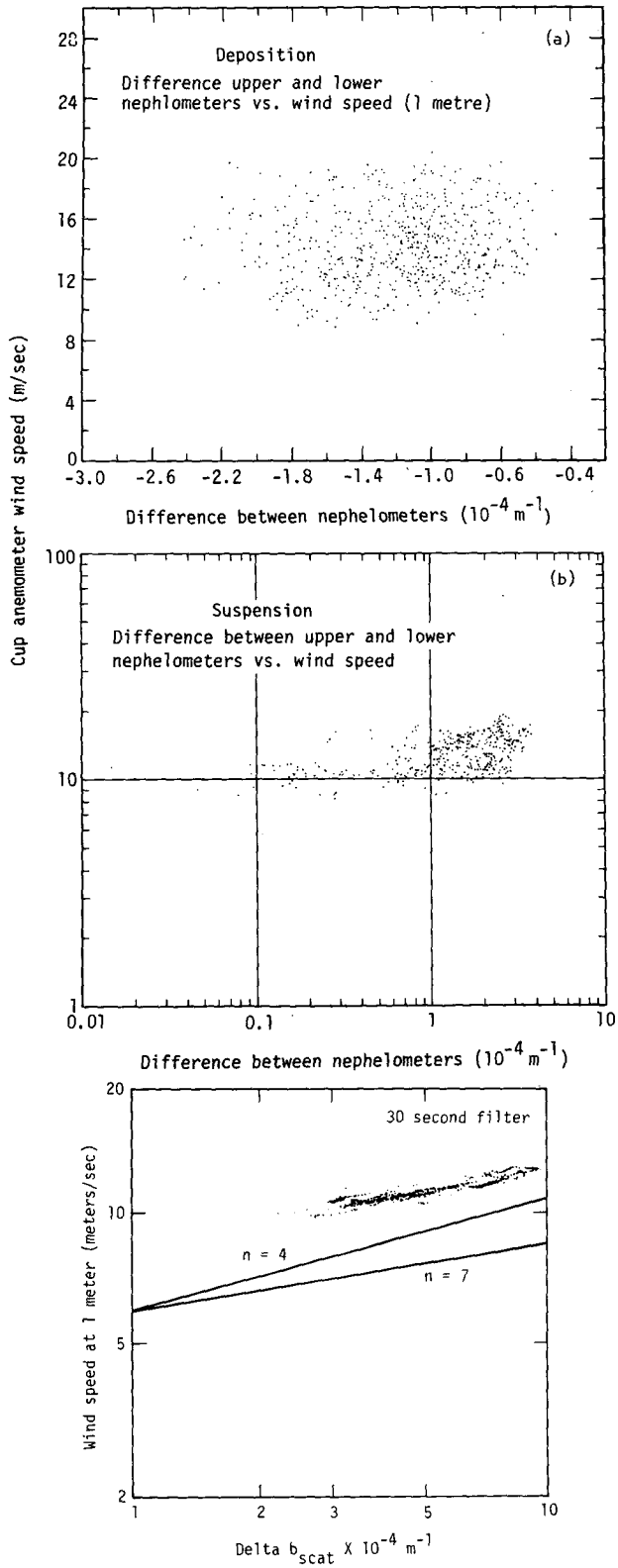

FIG. 4. Profile method determination of aerosol flux dependence on wind speed: (a) difference in nephelometer values at 1.4 and 5.1 m vs wind speed at 1 m for deposition period; (b) as in (a) except for suspension period; (c) previous years' data from a sandy soil for a 1 h period for nephelometer heights of 35.5 and 166 cm vs wind at 1 m.

for deposition velocity is

$$V_E=\frac{ku_*}{n[(z-d_p)/z_p]-\psi_p}, \tag{12}$$

where d_p and z_p are the zero-plane displacement and the roughness length of the quantity p, and z is the height of the measurement; ψ_p is a correction term which becomes important for a non-neutral atmosphere. Since our sampling took place in a nearly neutral atmosphere, we used values given in Hicks' paper for z_p for particles between 0.1 and 1 μm to give approximately

$$F_A=0.04u_*[C(z)-C(0)], \tag{13}$$

where $C(0)$ is the zero-plane concentration. Since the difference $C(z)-C(0)$ is less than $C(z)$ [possibly 30% of $C(z)$] (Gillette, 1974), comparison with Eq. (11) shows qualitative agreement. Indeed, the dependence of the expression of u_* agrees with our expression. However, the dependence of V_E on z/L, where L is the Monin-Obukhof length, and on z_p would indicate that our $F(x)$ should vary also with z/L (i.e., with height and atmospheric stability) as well as with roughness height. That is, $F=F(x,z/L,z_p)$.

Sehmel and Hodgson also approached the deposition velocity problem by the profile method. They computed deposition velocities as a function of atmospheric stability, roughness height, u_* and height. Their value for the deposition velocity for the conditions $u_*=50$ cm s^{-1}, $z_0=0.5$ cm, $z/L=0.0$, $z=1$ m and particle diameter ~ 1 μm is about 0.5 cm s^{-1}. Our value for the deposition velocity at 5.4 m for $u_*=40$ cm s^{-1} (approximately our observed value for u_*) with similar values for the other parameters is ~ 1.6 cm s^{-1} which is higher than the Sehmel and Hodgson values.

d. Spectral analysis

Spectral analysis of the wind and dust data also reveals much about the physical process we are observing. The theory of spectral analysis and application to meteorological parameters have been described in many papers (Bendat and Piersol, 1966; Lovill, 1970). The digital analysis technique was developed by Blackman and Tukey (1958) for numerically solving for the autospectral density (cross-spectral density) from the Fourier transform of the autocorrelation function (cross-correlation function). Since the auto- and cross-correlation functions are simply the functional covariances previously discussed and normalized by their standard deviations, the autospectral densities for parameters measured during the 6 min deposition period before the passage of the front. Fig. 7a is the spectrum for the vectorvane horizontal wind speeds at 5.4 m. Features which are immediately noticeable are the sharp peaks at 100 and 200 min^{-1} frequencies, a general slope close to the Kolmogorov slope of $-5/3$ derived for the inertial subrange, and high-frequency

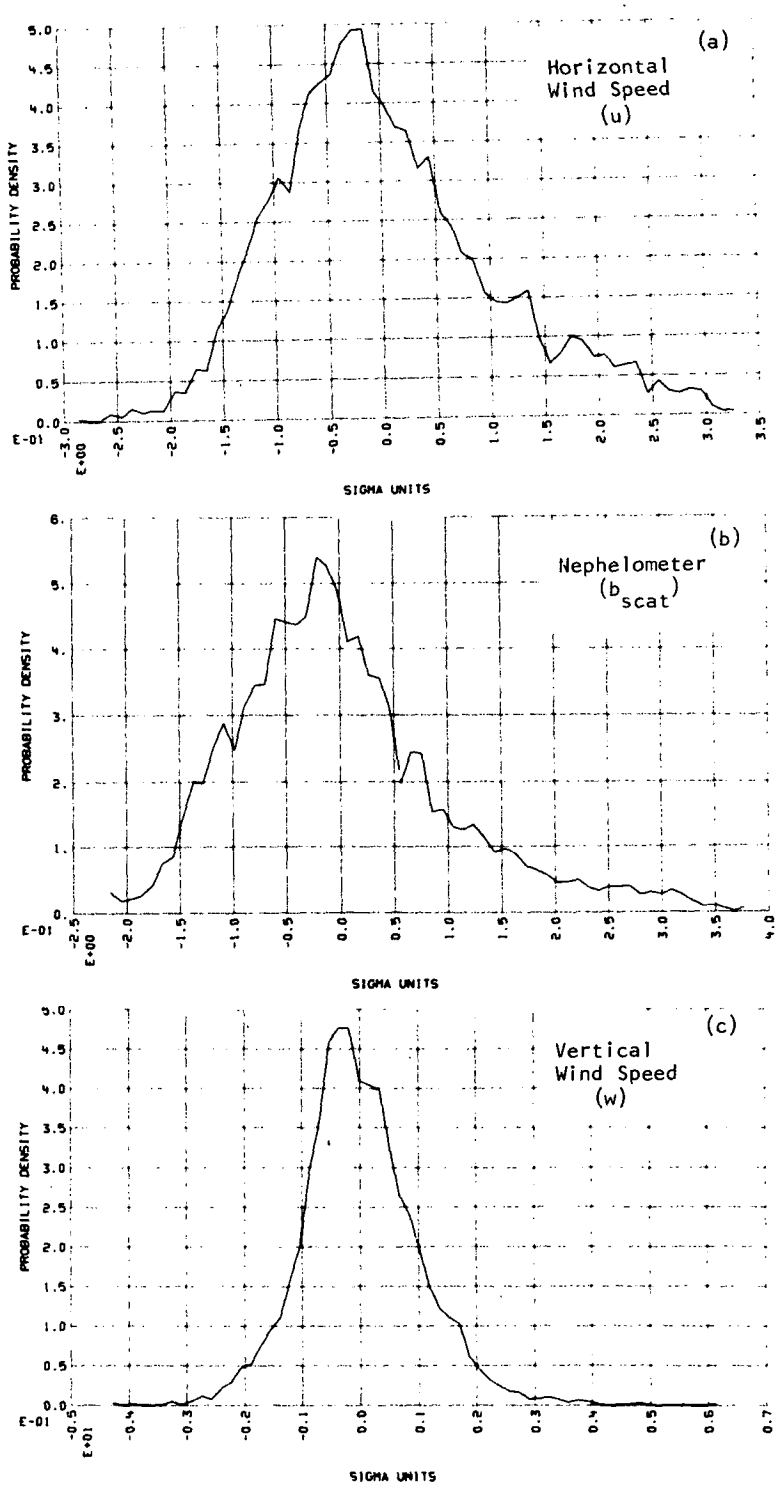

FIG. 5. Probability density versus sigma units for the three parameters u, b_{scat} and w measured at 5 m during the deposition period for the conditions shown in Fig. 1.

flattening at ~350 cpm (cycles per minute). Fig. 7a shows a very similar slope for the autospectral density of the light scattering data with a high-frequency flattening at ~300 cpm. The similarity of the shapes of these curves and the high-frequency flattening at ~5 Hz imply the speed of sampling criteria were met. The peaks at 100 and 200 Hz are due to data system effects and appear even on a disconnected channel. Their sharpness, however, precludes serious contribution to the total spectrum.

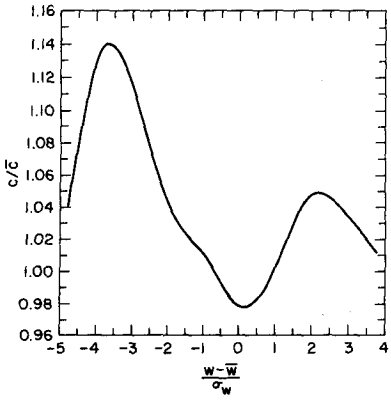

FIG. 6. Plot of $F(x)=b_{scat}(x)/\overline{b_{scat}}$ vs x, where x is $(w-\bar{w})/\sigma_w$. When combined with the data illustrated in Fig. 5 and numerically integrated, a constant of proportionality to the deposition velocity can be derived.

5. Conclusions

A fortunate meteorological situation and a site with fast-response aerosol and wind instrumentation allowed us to analyze deposition and suspension as separate phenomena on the same data record. The major results of this analysis can be summarized for particles with radii between 0.1 and 1 μm as follows:

1) Application of both the profile and covariance techniques for flux determination allows us to determine an approximate equivalence between the aerosol exchange coefficient K_A and the eddy viscosity K_M for the size distribution sampled.

2) The deposition velocity technique for flux determination yielded results comparable to values found from earlier work.

3) The size distribution of the soil particulates and the geometrical orientation of plowed furrows to the wind are important to the threshold velocity for suspension of particles from bare soil.

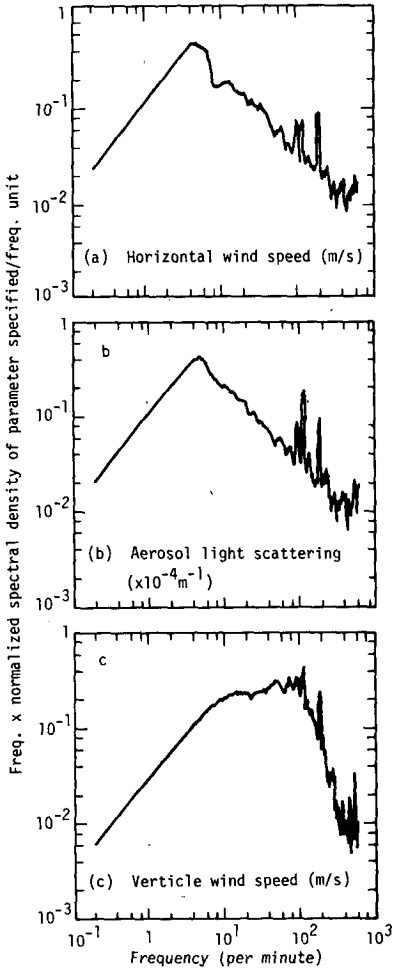

FIG. 7. Normalized autospectral densities for parameters shown in Fig. 5 measured during the 5 min deposition period.

Acknowledgments. The authors would like to thank Messrs. Gerald Dolan, Bob Dell and Greg Bianchini for their technical support during the experiment. Dr. Edward Patterson, Dr. James Lovill, Dr. David Ensor, Dr. Prem Bhardwaja, Dr. Bruce Hicks and Kendall Peterson gave many useful suggestions and Dr. Joseph Knox, Dr. Marvin Dickerson and Dr. Edwin Danielson for their support; and special thanks are due to Dr. Joseph Shinn who's design of the earlier experiment was invaluable to this work.

REFERENCES

Ahlquist, N. C., and R. J. Charlson, 1967: A new instrument for evaluating the visual quality of air. *Air Pollut. Control Assoc. J.*, **17**, 467–469.

Anspaugh, L. R., P. L. Phelps, N. C. Kennedy and H. G. Booth, 1973: Distribution and redistribution of airborne particulates from the Schooner Cratering event. Lawrence Livermore Laboratory Rep. UCRL-74392.

Aylor, D. E., 1976: Resuspension of particles from plant surfaces by wind. *ERDA Symp. Ser.*, No. 38, 791–812.

Bagnold, R. A., 1941: *The Physics of Blown Sand and Desert Dunes*, 1st ed. Chapman and Hall, 265 pp.

Bendat, J. S., and A. G. Piersol, 1966: *Measurement and Analysis of Random Data*. Wiley, 320 pp.

Blackman, R. B., and J. W. Tukey, 1958: *The Measurement of Power Spectra from the Point of View of Communications Engineering*. Dover, 190 pp.

Bortkovskij, R. S., 1972: On the mechanism of ocean-atmosphere interaction during a gale. *Tr. Geofiz. Observ. T. Vyp.*, No. 282, 187–193.

Buoycous, G. J., 1951: A recalibration of the hydrometer method for making mechanical analyses of soils. *Agron. J.*, **43**, 434–438.

Businger, J. A., 1965: Eddy diffusion and settling speed in blown snow. *J. Geophys. Res.*, **70**, 3307–3313.

Carlson, T. N., J. M. Prospero and K. J. Hanson, 1973: Attenuation of solar radiation by wind borne Saharan dust off the west coast of Africa. NOAA Tech. Memo ERL-WMPO-7, 27 pp.

Chepil, W. S., 1957: Sedimentary characteristics of dust storms. *Amer. J. Sci.*, **255**, 12–22.

Ensor, D. S., and A. P. Waggoner, 1970: Angular truncation error in the integrating nephelometer. *Atmos. Environ.*, **4**, 481–487.

Gillette, D. A., 1974: On the production of soil wind erosion

aerosols having the potential for long range transport. *J. Rech. Atmos.*, 735–744.

——, 1976: Production of fine dust by wind erosion of soil-effect of wind and soil texture. *ERDA Symp. Ser.*, No. 38, 591–609.

——, I. H. Blifford, Jr. and C. R. Fenster, 1972: Measurements of aerosol size distributions and vertical fluxes of aerosols on land subject to wind erosion. *J. Appl. Meteor.*, **11**, 977–987.

Hagen, L. J., and N. P. Woodruff, 1973: Air pollution from dust storms in the Great Plains. *Atmos. Environ.*, **7**, 323–332.

Harrison, P. R., R. G. Draftz and W. H. Murphy, 1976: Identification and impact of Chicago's ambient suspended dust. *ERDA Symp. Ser.*, No. 38, 540–556.

Heathershaw, A. D., 1974: Bursting phenomena in the sea. *Nature*, **248**, 394–395.

Hicks, B., 1976: Some micrometeorological aspects of pollutant deposition rates near the surface. Atmospheric-Surface Exchange of Particulate and Gaseous Pollutants-1974, ERDA, CONF-740921, 434–449.

Kaimal, J. C., 1975: Sensors and techniques for direct measurement of turbulent fluxes and profiles in the atmospheric surface layer. *Atmos. Tech.*, No. 7, 7–23.

Laktionov, A. G., 1967: Aspiration of an aerosol into a vertical tube from a flow transverse to it. *Fiz. Aeroz. Eksper. Usl. Pri.*, No. 7, 83–87.

Lumley, J. L., and H. A. Panofsky, 1964: *The Structure of Atmospheric Turbulence.* Wiley-Interscience, 239 pp.

Lovill, J. E., 1970: Dynamics of the structure of the atmosphere (ozone measurements). Atmos. Sci. Paper No. 160, Colorado State University, 51 pp.

Mellor, M., 1965: Blowing snow. Part III, Section A3c, U. S. Army Material Command, CRREL, Hanover, N. H.

Newman, J. E., M. D. Abel, W. A. Bruns, and K. J. Yost, 1974: Some atmospheric transport characteristics of suspended particles and associated trace contaminants around the south end of Lake Michigan. Lawrence Berkeley Laboratory Rep. LBL-3217, 103 pp.

Patterson, E. M., D. A. Gillette and G. W. Grams, 1976: The relation between visibility and the size-number distribution of airborne soil particles. *J. Appl. Meteor.*, **15**, 470–478.

Porch, W. M., and J. H. Shinn, 1976: Fast-response light scattering measurements of the characteristics of wind suspended aerosols. *ERDA Symp. Ser.*, No. 38, 610–624.

Punjrath, J. A., and D. R. Heldman, 1972: Influence of air turbulence on re-entrainment of small particles from flat surfaces. *Trans. Amer. Soc. Agric. Eng.*, 559–562.

Raynor, G. S., 1976: Experimental studies of pollen deposition to vegetated surfaces. *ERDA Symp. Ser.*, No. 38, 264–279.

Sehmel, G. A., and W. H. Hodgson, 1976: Predicted dry deposition velocities. Atmospheric-Surface Exchange of Particulate and Gaseous Pollutants-1974, ERDA, CONF-740921, 399–422.

——, and F. D. Lloyd, 1976: Resuspension of plutonium at Rocky Flats. *ERDA Symp. Ser.*, No. 38, 757–779.

Shinn, J. H., N. C. Kennedy, J. S. Koval, B. R. Clegg and W. M. Porch, 1976: Observations of dust flux in the surface boundary layer for steady and non-steady cases. *ERDA Symp. Ser.*, No. 38, 625–637.

Skidmore, E. L., 1974: A wind erosion equation: Development, application and limitations. *ERDA Symp. Ser.*, No. 38, 452–465.

Wyngaard, J. C., O. Coté and Y. Izumi, 1971: Local free convection, similarity and budgets of shear stress and heat flux. *J. Atmos. Sci.*, **28**, 1171–1182.